Basic Sizing of Aircraft Structural Elements

M.Drela 4 Oct 2022

Nomenclature

A	structural member area
$\mathcal{A}$	shell enclosed area
b	span
c	chord
C_L	aircraft lift coefficient
c_m	local pitching moment coefficient
E	stiffness modulus
G	shear modulus
h	spar height
I	bending moment of inertia
J	torsion moment of inertia
L	lift
ℓ	length
$\mathcal{M}$	bending moment
N	flight load factor ($= L/W_{\mathrm{total}}$)
N_{land}	landing load factor ($= a_z/g$)
$\mathcal{P}$	axial load
p	net transverse load per length
q	flight dynamic pressure ($= \frac{1}{2}\rho_\infty V^2$)
R	tube radius
S	reference area (wing area $\int c \, \mathrm{d}y$)
$\mathcal{S}$	shear
$\mathcal{T}$	torsion moment
t	wall thickness
V	airspeed
W	weight
y	spanwise coordinate
w	bending deflection

α	angle of attack
η	spanwise coordinate ($= 2y/b$)
θ	bending angle ($= \mathrm{d}w/\mathrm{d}y$)
κ	bending curvature ($= \mathrm{d}^2 w/\mathrm{d}y^2$)
λ	taper ratio ($= c_{\mathrm{tip}}/c_0$)
ρ	material density
σ	axial stress
τ	shear stress
ϕ	twist angle

$(\,)_0$	quantity at wing center $y = 0$
$(\,)_{\mathrm{tip}}$	quantity at wing tip $y = b/2$
$(\,)'$	quantity per unit span ($= \mathrm{d}(\,)/\mathrm{d}y$)
$(\,)_{\mathrm{max}}$	max specified or allowable quantity
$(\,)_{NE}$	never-exceed quantity

1 Load Cases

Each structural element is typically sized by the load it must carry at a specific *load case*. Some common load cases which size typical aircraft structural elements are listed below.

Element	Criterion	Parameter	Sizing load case
spar cap area	strength	σ_{max}	N_{max}
spar cap area	strength	σ_{max}	N_{land}
spar cap area	stiffness	$(w_{\mathrm{tip}}/b)_{\mathrm{max}}$	N_{max}
spar web area	strength	τ_{max}	N_{max}
wing skin thickness	strength	τ_{max}	aileron deflection at V_{NE}
wing skin thickness	stiffness	$(\phi_{\mathrm{tip}})_{\mathrm{max}}$	aileron deflection at V_{NE}
tailboom wall thickness	strength	σ_{max}	max vertical tail load at V_{NE}
tailboom wall thickness	stiffness	$\mathrm{d}\theta/\mathrm{d}\alpha$	α perturbation at V_{NE}

Each load case has a corresponding load diagram which determines the tension, shear, torsion moment, or bending moment and corresponding stress and strain in the structural element. For the wing load case shown in Figure 1, the net effective load distribution on the wing is the aerodynamic lift minus the weight and inertial reaction,

$$p(y) \;=\; L'(y) \;-\; N W'_{\mathrm{wing}}(y) \tag{1}$$

which then results in the following shear and moment distributions.

$$\mathcal{S}(y) \;=\; \int_y^{b/2} p \; \mathrm{d}y \qquad\qquad \mathcal{M}(y) \;=\; \int_y^{b/2} \mathcal{S} \; \mathrm{d}y \tag{2}$$

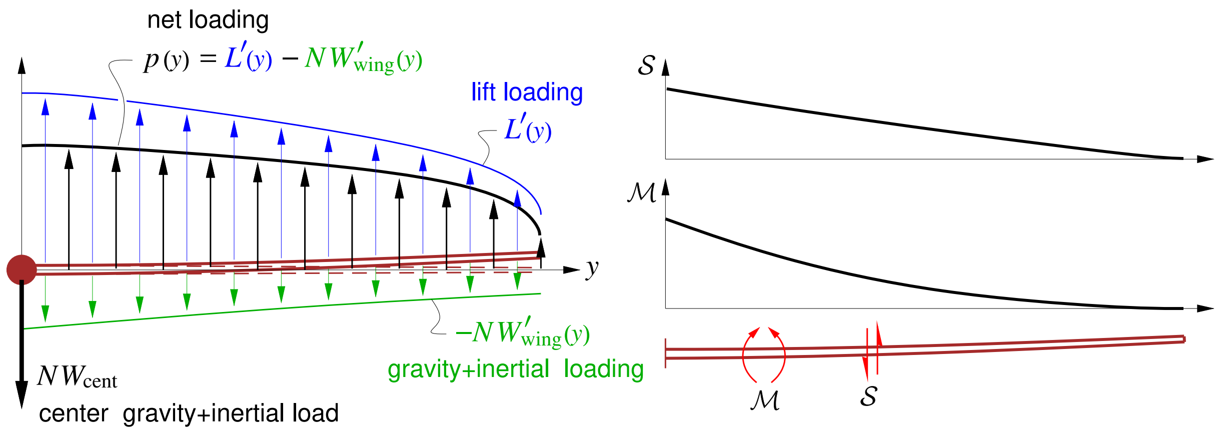

Figure 1: Flight wing loads and resulting shear and bending moment distributions.

It's useful to note that the integral of the net loading $p(y)$ over the entire span is equal to the load factor times the central weight.

$$\int_{-b/2}^{b/2} p \; \mathrm{d}y \;=\; \int_{-b/2}^{b/2} \left(L' - NW'_{\text{wing}}\right) \mathrm{d}y \;=\; N\left(W_{\text{total}} - W_{\text{wing}}\right) \;=\; N\,W_{\text{cent}} \tag{3}$$

Hence, the structural loads on the wing are determined mainly by the center weight, which excludes the weight of the wing itself, $W_{\text{cent}} = W_{\text{total}} - W_{\text{wing}}$.

2 Spar Sizing

The spar being sized consists of top and bottom sparcaps which are assumed to carry the entire bending moment $\mathcal{M}$, and a shear web with a composite skin which is assumed to carry the entire shear load $\mathcal{S}$. The spar may also be filled with a core which carries no significant load.

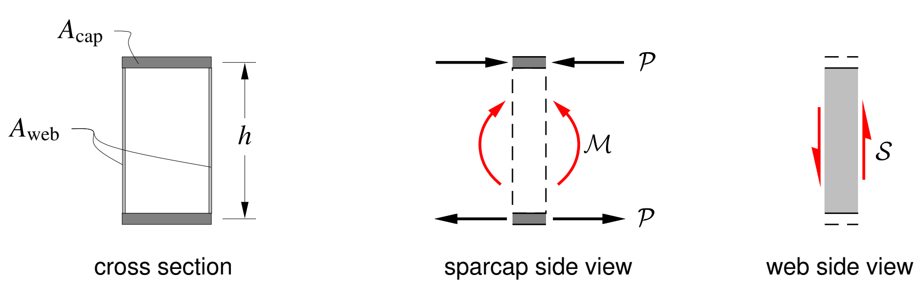

Figure 2: Spar cross section, and side views with sparcap and web loads.

2.1 Spar loads

The structural analysis is considerably simplified if we make the assumption that the net loading is proportional to the local chord,

$$p(y) \;\simeq\; K_p\, c(y) \tag{4}$$

and substituting this into (3) gives the value of the proportionality constant.

$$K_p \;=\; \frac{N\,W_{\rm cent}}{S} \tag{5}$$

For a straight-taper wing with taper ratio $c_{\rm tip}/c_0 = \lambda$, the chord distribution is

$$c(y) \;=\; \frac{S}{b}\frac{2}{1{+}\lambda}\left[\,1\,+\,(\lambda{-}1)\,\eta\,\right] \tag{6}$$

and the corresponding root shear and bending moments can then be obtained explicitly.

$$\mathcal{S}_0 \;=\; \mathcal{S}(0) \;=\; \frac{NW_{\rm cent}}{2} \tag{7}$$

$$\mathcal{M}_0 \;=\; \mathcal{M}(0) \;=\; \frac{NW_{\rm cent}\,b}{12}\,\frac{1{+}2\lambda}{1{+}\lambda} \tag{8}$$

2.2 Spar strength sizing

The sparcap load resulting from some bending moment is

$$\mathcal{P} \;=\; \frac{\mathcal{M}}{h} \;=\; \sigma\,A_{\rm cap} \tag{9}$$

and this is also the product of the sparcap stress and area as given above. The latter relation assumes the sparcap is very thin relative to the spar height h, so that the sparcap stress is then nearly uniform. The sparcap area at the wing root is then determined such that the stress is at its max allowable value at the maximum wing load case.

$$\boxed{A_{{\rm cap}_0} \;=\; \frac{N_{\rm max}W_{\rm cent}}{12\,\sigma_{\rm max}}\,\frac{b}{h}\,\frac{1{+}2\lambda}{1{+}\lambda}} \tag{10}$$

The spar web shear load is carried by the web shear stress,

$$\mathcal{S} \;=\; \tau\,A_{\rm web} \tag{11}$$

which then gives the required web area (of all webs present) at the maximum wing load case.

$$\boxed{A_{{\rm web}_0} \;=\; \frac{N_{\rm max}W_{\rm cent}}{2\,\tau_{\rm max}}} \tag{12}$$

The optimum sparcap and web area variation across the span, $A_{\rm cap}(y)$ and $A_{\rm web}(y)$, is obtained by applying the sizing criteria (10) and (12) to each spanwise location using the local $\mathcal{M}(y)$, $\mathcal{S}(y)$, and $h(y)$ values. A simpler approach is to obtain these by scaling the root values, with the assumptions that $\mathcal{M}$ drops quadratically and $\mathcal{S}$ drops linearly towards the tip, as suggested by the diagrams in Figure 1.

$$A_{\rm cap}(y) \;=\; A_{{\rm cap}_0}\,(1{-}\eta)^2 \tag{13}$$

$$A_{\rm web}(y) \;=\; A_{{\rm web}_0}\,(1{-}\eta) \tag{14}$$

This is correct for a uniform spanwise loading (e.g. an untapered wing), and somewhat conservative for a tapered wing.

2.3 Spar stiffness sizing

Assuming the spar is sized so as to have roughly uniform stresses across the span (i.e. the spar caps are tapered appropriately), then the spar bending curvature can be assumed to be roughly uniform, and equal to its center value,

$$\frac{\mathrm{d}^2 w}{\mathrm{d}y^2} = \kappa(y) \simeq \kappa_0 = \frac{\mathcal{M}_0}{EI_0} \tag{15}$$

$$I_0 = \frac{A_{\mathrm{cap}_0}\, h^2}{2} \tag{16}$$

where the bending inertia of the spar cross section I_0 ignores any contributions from the web. The corresponding approximate deflection angle distribution and tip bending deflection can then be computed explicitly.

$$\theta(y) = \int_0^y \kappa_0 \, \mathrm{d}y = \kappa_0\, y \tag{17}$$

$$w(y) = \int_0^y \theta \, \mathrm{d}y = \frac{\kappa_0\, y^2}{2} \tag{18}$$

$$w_{\mathrm{tip}} = w(b/2) = \frac{\kappa_0\, b^2}{8} \tag{19}$$

A stiffness constraint will typically impose a maximum deflection to span ratio, $(w_{\mathrm{tip}}/b)_{\mathrm{max}}$, which then gives the required center sparcap area by rearranging (19).

$$\boxed{A_{\mathrm{cap}_0} = \frac{NW_{\mathrm{cent}}}{48\,E} \, \frac{b^2}{h^2} \, \frac{1}{(w_{\mathrm{tip}}/b)_{\mathrm{max}}} \, \frac{1+2\lambda}{1+\lambda}} \tag{20}$$

The simple taper approximation (13) is also appropriate here to obtain the spanwise sparcap area distribution.

3 Wing Skin Sizing

A major structural function of the wing skin is to provide torsional strength and stiffness against a torsion load whose greatest value is typically is imposed by the maximum aileron deflection at the never-exceed speed. The local torsion moment is

$$\mathcal{T}(y) = \int_y^{b/2} q\, c^2\, c_m \, \mathrm{d}y \tag{21}$$

which depends on the $c(y)$ and $c_m(y)$ distributions. One limiting case is if the pitching moment is concentrated only over an aileron which has some limited span b_{ail} and is centered at spanwise location y_{ail} as diagrammed in Figure 3. In this case the torsion inboard of the aileron is constant and is

$$\mathcal{T} = q\, b_{\mathrm{ail}}\, c_{\mathrm{ail}}^2\, c_m \tag{22}$$

where c_{ail} is the wing chord at the aileron location.

Regardless of the $\mathcal{T}(y)$ distribution over the span, the skin has a local shear stress given by

$$\tau = \frac{\mathcal{T}}{2\mathcal{A}\, t} \tag{23}$$

where $\mathcal{A}(y)$ is the local area enclosed by the shell, and $t(y)$ is the local skin thickness, as shown in Figure 4.

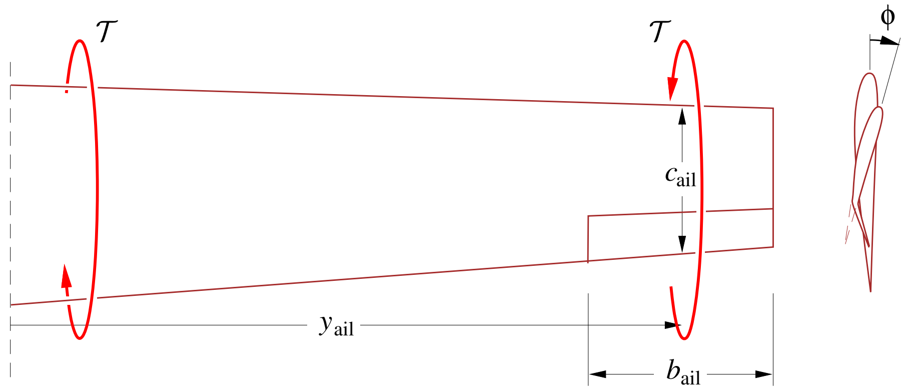

Figure 3: Wing twist from torsion load of deflected aileron.

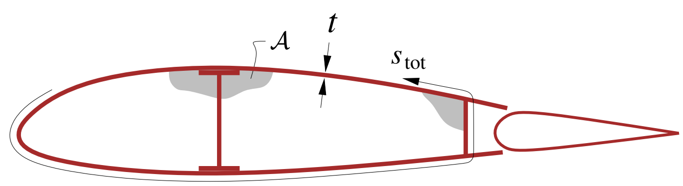

Figure 4: Torsion shell parameters of a wing cross section.

3.1 Skin strength sizing

The required wing skin thickness at any location can be determined directly from equation (23) by imposing a maximum tolerable shear stress at the never-exceed condition.

$$\boxed{t(y) \;=\; q_{NE}\, b_{\text{ail}}\, c_{\text{ail}}^2\, c_m \,\frac{1}{2\mathcal{A}}\,\frac{1}{\tau_{\max}}} \tag{24}$$

This will be greatest where $A(y)$ is a minimum.

3.2 Skin stiffness sizing

The local torsional stiffness of a closed thin-walled section with a uniform wall thickness t is

$$J(y) \;\simeq\; \frac{4\mathcal{A}^2\, t}{s_{\text{tot}}} \tag{25}$$

where $s_{\text{tot}}(y)$ is the perimeter of the shell cross section. The twist rate from an applied torsion moment $\mathcal{T}$ is

$$\phi'(y) \;=\; \frac{\mathcal{T}}{GJ} \tag{26}$$

where G is the skin material's shear modulus. The tip twist angle is then

$$\phi_{\text{tip}} \;=\; \int_0^{y_{\text{ail}}} \frac{\mathcal{T}}{GJ}\, \mathrm{d}y \;=\; \mathcal{T}\left(\frac{1}{GJ}\right)_{\text{avg}} y_{\text{ail}} \tag{27}$$

where y_{ail} is the spanwise location of the aileron midpoint. The second form above uses the spanwise-averaged torsional compliance, which is the inverse of GJ. For an untapered wing with a spanwise-constant $\mathcal{A}$, t, and J, the required skin thickness can be obtained from equation (27) by imposing a maximum tolerable tip twist angle $(\phi_{\rm tip})_{\rm max}$ at the never-exceed condition.

$$\boxed{t \;=\; q_{\scriptscriptstyle NE}\, b_{\rm ail}\, c_{\rm ail}^2\, y_{\rm ail}\, c_m \, \frac{s_{\rm tot}}{4\mathcal{A}^2 G} \, \frac{1}{(\phi_{\rm tip})_{\rm max}}} \tag{28}$$

For a tapered wing, the appropriate $t(y)$ variation across the span may need to be determined iteratively by repeated computation of the twist angle using the integration in (27).

A more complete analysis of a torsion shell with multiple cells, such as the one shown in Figure 4, is actually considerably more involved. However, since the torsional stiffness for a given shell thickness is always increased by multiple cells, using the much simpler single-cell results above is conservative and usually adequate for preliminary design.

4 Tube Sizing

A hollow tube is the most weight-efficient form for carrying torsion loads. However, since tubes are commercially available in a large variety of sizes and materials, they are frequently also used as compression and bending structural members for cost and convenience reasons.

The wall thickness and wall area, and the bending and torsion inertias of a tube are

$$t \;=\; R_{\rm outer} - R_{\rm inner} \tag{29}$$

$$A \;=\; \pi \left(R_{\rm outer}^2 - R_{\rm inner}^2 \right) \;\simeq\; 2\pi\, R_{\rm outer}\, t \tag{30}$$

$$I \;=\; \frac{\pi}{4} \left(R_{\rm outer}^4 - R_{\rm inner}^4 \right) \;\simeq\; \pi\, R_{\rm outer}^3\, t \;\simeq\; \frac{1}{2} A\, R_{\rm outer}^2 \tag{31}$$

$$J \;=\; \frac{\pi}{2} \left(R_{\rm outer}^4 - R_{\rm inner}^4 \right) \;\simeq\; 2\pi\, R_{\rm outer}^3\, t \;\simeq\; A\, R_{\rm outer}^2 \tag{32}$$

where each approximate expression assumes a small wall thickness relative to the outer radius, $t/R_{\rm outer} = 1 - R_{\rm inner}/R_{\rm outer} \ll 1$.

4.1 Tube torsion strength sizing

The shear stress at the tube's outer radius resulting from an applied torsion moment $\mathcal{T}$ is

$$\tau \;=\; \frac{\mathcal{T} R_{\rm outer}}{J} \;\simeq\; \frac{\mathcal{T}}{2\pi R_{\rm outer}^2 t} \tag{33}$$

where the second approximate form assumes a small wall thickness. This expression then gives the required thickness needed to carry a given maximum torsion load without exceeding the tube material's maximum allowable shear stress.

$$\boxed{t \;=\; \frac{\mathcal{T}_{\rm max}}{2\pi R_{\rm outer}^2 \tau_{\rm max}}} \tag{34}$$

The corresponding weight of the tube of some length ℓ is

$$W \;=\; \rho g\, A\, \ell \;=\; \rho g \, \frac{\mathcal{T}_{\rm max}\, \ell}{R_{\rm outer}\, \tau_{\rm max}} \tag{35}$$

which scales inversely with the tube outer radius, and therefore favors very large radius and very thin wall tubes. In practice, the tube radius is always limited by space, shell buckling, damage tolerance, a minimum-gauge limit on t, or by commercial availability.

4.2 Tube torsion stiffness sizing

The overall twist angle over the length ℓ of the tube under torsion is

$$\Delta\phi \;=\; \frac{\mathcal{T}\ell}{GJ} \tag{36}$$

which is equivalent to the wing twist given by (27) and pictured in Figure 3. The required wall thickness via the approximate J formula in (32) is then

$$\boxed{t \;=\; \frac{\mathcal{T}_{\max}\,\ell}{2\pi R_{\text{outer}}^3\, G}} \tag{37}$$

and the corresponding weight is

$$W \;=\; \rho g\, A\,\ell \;=\; \rho g\, \frac{\mathcal{T}_{\max}\,\ell^2}{R_{\text{outer}}^2\, G} \tag{38}$$

which scales inversely with the square of the radius, and therefore favors a large tube radius even more than in the strength-sizing case. The same limits on the maximum tube radius apply here also.

4.3 Tube bending strength sizing

The maximum axial stress in the tube resulting from an applied bending moment $\mathcal{M}$ is

$$\sigma \;=\; \frac{\mathcal{M} R_{\text{outer}}}{I} \;\simeq\; \frac{\mathcal{M}}{\pi R_{\text{outer}}^2 t} \tag{39}$$

where again the second approximate form assumes a small wall thickness. The required thickness needed to carry a given maximum bending moment and the corresponding tube weight then follow.

$$\boxed{t \;=\; \frac{\mathcal{M}_{\max}}{\pi R_{\text{outer}}^2 \sigma_{\max}}} \tag{40}$$

$$W \;=\; \rho g\, A\,\ell \;=\; \rho g\, \frac{2\mathcal{M}_{\max}\,\ell}{R_{\text{outer}}\,\sigma_{\max}} \tag{41}$$

The considerations for choosing the tube radius are the same as in the torsion case.

4.4 Tube bending deflection sizing

The tube's local bending curvature is given by the following general beam relation.

$$\kappa(y) \;=\; \frac{\mathcal{M}}{EI} \;\simeq\; \frac{\mathcal{M}}{\pi R_{\text{outer}}^3\, t\, E} \tag{42}$$

Typically the tube of length ℓ is a cantilever clamped at one end, and the bending moment distribution $\mathcal{M}(y)$ is the result of an applied transverse load $\mathcal{F}$, either concentrated or distributed over the tube in some manner. In general, all loading cases give the free-end deflection and deflection angle as

$$w(\ell) \;=\; \frac{k_\delta\, \mathcal{F}\ell^3}{EI} \;=\; \frac{k_\delta\, \mathcal{F}\ell^3}{\pi R_{\text{outer}}^3\, t\, E} \tag{43}$$

$$\theta(\ell) \;=\; \frac{k_\theta\, \mathcal{F}\ell^2}{EI} \;=\; \frac{k_\theta\, \mathcal{F}\ell^2}{\pi R_{\text{outer}}^3\, t\, E} \tag{44}$$

where the constants k depend on the distribution of the total load $\mathcal{F}$. Two particular cases are:

$$\begin{aligned} k_\delta &= \tfrac{1}{3} \quad , \quad k_\theta = \tfrac{1}{2} \quad , \quad \text{load } \mathcal{F} \text{ concentrated at free end at } y=\ell \\ k_\delta &= \tfrac{1}{8} \quad , \quad k_\theta = \tfrac{1}{6} \quad , \quad \text{load } \mathcal{F} \text{ distributed uniformly over } y = 0 \ldots \ell \end{aligned} \tag{45}$$

The tip deflection result (43) can be recast into a requirement of the wall thickness if the maximum allowable deflection $w_{\max}$ is specified at the maximum expected load.

$$\boxed{t \;=\; \frac{k_\delta\, \mathcal{F}_{\max}\, \ell^3}{\pi R_{\text{outer}}^2 w_{\max} E}} \tag{46}$$

The tip deflection angle result (44) can be recast into an alternative requirement on the maximum allowable angle $\theta_{\max}$.

$$\boxed{t \;=\; \frac{k_\theta\, \mathcal{F}_{\max}\, \ell^2}{\pi R_{\text{outer}}^2 \theta_{\max} E}} \tag{47}$$

4.5 Tube column buckling sizing

If the tube is subjected to an axial compressive load $\mathcal{P}$, it will buckle if this exceeds the critical load given by

$$\mathcal{P}_{\text{cr}} \;=\; C\,\frac{\pi^2 EI}{\ell^2} \tag{48}$$

where the end fixity parameter C depends on how the tube ends are supported. The values of C for four particular end support cases are shown in Figure 5.

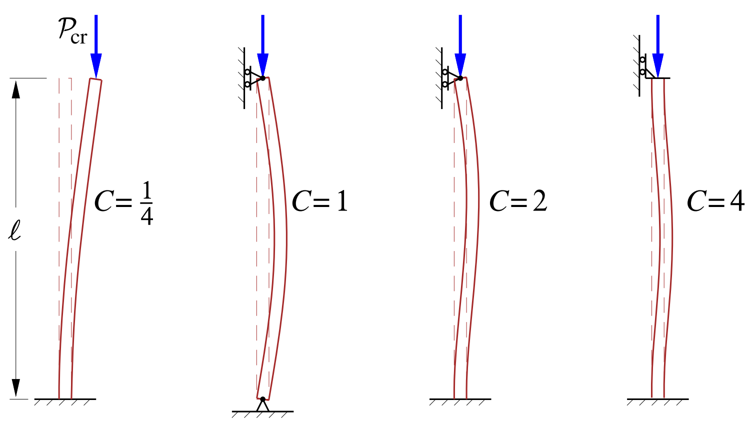

Figure 5: Column buckling with four end-support cases.

The buckling load expression above can be recast into a requirement for the tube wall thickness at the maximum anticipated compressive load.

$$\boxed{t \;=\; \frac{1}{C}\,\frac{\mathcal{P}_{\max}\, \ell^2}{\pi^3 R_{\text{outer}}^3 E}} \tag{49}$$

Since end supports cannot be perfectly rigid, the largest fixity value $C = 4$ is not realizable in practice. Also, the critical buckling load can decrease dramatically from its theoretical value given by (48) if it is applied even slightly off the tube's centerline. This suggests that a significant margin of safety is appropriate when choosing the tube wall thickness by the buckling criterion.

5 Mechanical Design Considerations

Good mechanical design as a minimum requires consideration of the critical load cases and material properties, as used in the sizing relations and procedures given above. However, each of these relations applies only to a specific type of the structural member, such as an I-beam spar, torsion shaft, or compression column. How these members are selected and combined into an overall structure falls under the more general art of mechanical design, which involves other considerations such as

- Load path topology
- Manufacturability
- Durability and damage tolerance
- Cost

and possibly others. This section will focus mainly on load path topology.

5.1 Reaction loads

As dictated by Newton's 3rd Law, every load on an object has an equal and opposite *reaction load* somewhere else on the object. A reaction load can be either

- another applied load, or
- an inertial-reaction load, on accelerating mass.

Specifically, an item with mass m_i undergoing acceleration $\mathbf{a}$ imparts an inertial reaction load $\mathbf{F}_i = -m_i\mathbf{a}$ to the structure, as shown in the rocket example in Figure 6.

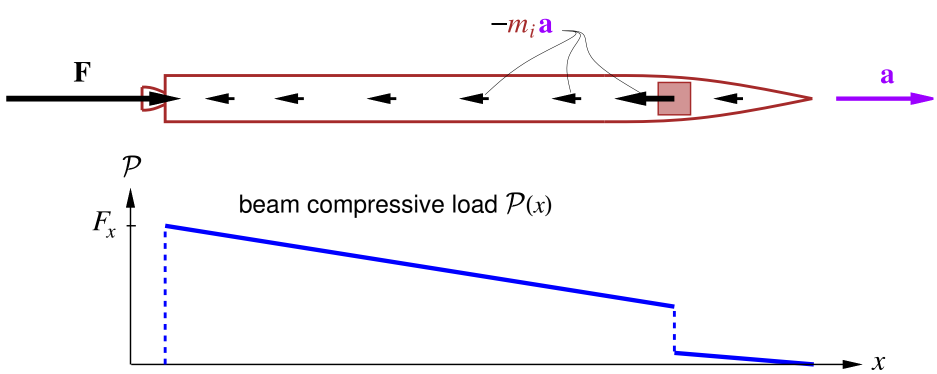

Figure 6: Applied and reaction loads on rocket, and resulting axial load diagram

Reaction loads occur only if the applied loads have a nonzero sum, which produces the necessary nonzero body acceleration. Linear acceleration is uniform over the body, while centripetal acceleration due to rotation varies radially over the body. In any case, it's useful to note that the summed applied+inertial load sum always vanishes,

$$\begin{aligned}
\mathbf{F} + \textstyle\sum_i \mathbf{F}_i &= \mathbf{F} + \textstyle\sum_i m_i\,\mathbf{a} \\
&= \mathbf{F} - m\,\mathbf{a} \\
&= \mathbf{0}
\end{aligned} \tag{50}$$

which is a useful check on the assumed load distribution.

Reaction loads are in general distributed over the body mass, although for a compact mass they can be idealized as a point load. All the loads together can then be used to produce a suitable load diagram, as for example shown in Figure 6. The defining relation for the compressive load in the rocket case in Figure 6 is

$$\mathcal{P}(x) \;=\; \int^{x} f_x(x')\,\mathrm{d}x' \tag{51}$$

where $f_x(x)$ is the total (applied+inertial) load/length distribution in the x direction. A concentrated load is an f_x impulse, producing a jump in $\mathcal{P}(x)$, as sketched.

5.2 Load paths

A *load path* is the structural material which carries or transmits, via its internal stresses, the force from the applied to the reaction load locations. At the design stage, different alternative load paths and corresponding structural shapes are possible, and choosing the best one is one of the objectives of mechanical design

The lowest amount of stressed material, and hence the lowest structural weight, is obtained with the shortest possible load path (or paths if multiple applied or reaction loads are being considered). Figure 7 shows straight and bent load paths between the same applied loads, with the bent path having much larger local material loads which in this case is attributable to the opposing material loads associated with bending moments. The larger loads then demand more stressed material and result in a larger structural mass.

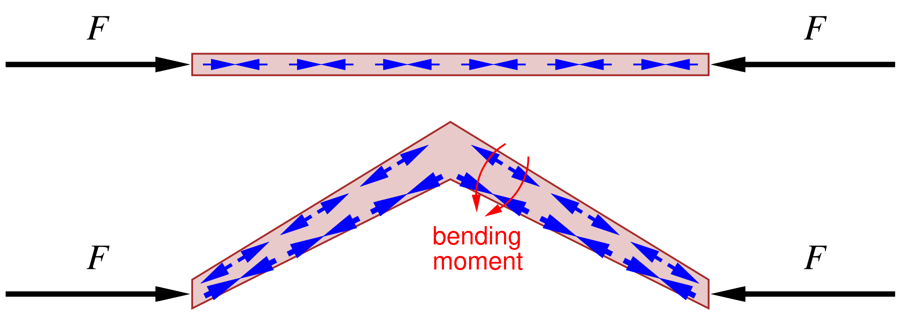

Figure 7: Straight and bent load paths between applied and reaction loads, with material stresses indicated in blue. Bent path has larger opposing material loads associated with bending moments

In aircraft structural design, choosing the best load path often involves a weight/drag tradeoff. For example, the most direct load path between the fuselage weight and the lift centroid on each wing half is a straight diagonal strut, diagrammed in the top of Figure 8. However, this would require an external strut which carries an aerodynamic drag penalty. Note that this also produces some compression load on the wing. Putting the load path inside the fuselage and the wing, as shown in the bottom of Figure 8, eliminates the external strut drag, but produces much larger opposing compression/tension loads (bending moments) in the wing which require more structural material and more weight.

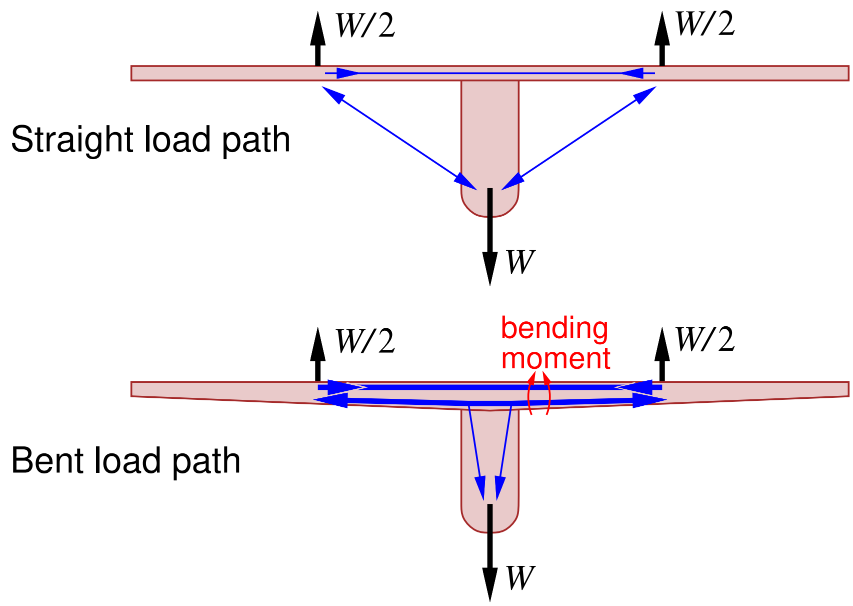

Figure 8: Direct and bent load paths between applied fuselage weight and reacting wing lift loads. The direct path has and external strut and hence a drag penalty, while the bent path produces wing bending moments which results in a structural weight penalty.